Available online at www.sciencedirect.com
ScienceDirect
Thermochimica Acta 456 (2007) 114–119
thermochimica acta
www.elsevier.com/locate/tca

Solid–liquid equilibria of three binary systems: {1-Ethyl-3-methylimidazolium hexafluorophosphate + 2-phenylimidazole, or 4,5-diphenylimidazole or 2,4,5-triphenylimidazole}

Hocine Sifaoui[a], Ahmed Ait-Kaci[a], Ali Modarressi[b], Marek Rogalski[b,*]

[a] *Laboratoire de Thermodynamique et de Modélisation Moléculaire, Faculté de Chimie, USTHB, BP 32 El-Alia, 16111 Bab-Ezzouar, Alger, Algeria*
[b] *Laboratoire de Chimie et Applications, IPEM, Université Paul Verlaine de Metz, 1 Boulevard Arago, 57070 Technopole, Metz, France*

Received 16 November 2006; received in revised form 18 January 2007; accepted 8 February 2007
Available online 16 February 2007

Abstract

The phase diagrams of binary mixtures formed by 1-ethyl-3-methylimidazolium hexafluorophosphate ([emim][PF_6]) and 2-phenylimidazole or 4,5-diphenylimidazole or 2,4,5-triphenylimidazole has been established using differential scanning calorimetry. Solutions containing 2,4,5-triphenylimidazole display phase splitting at high temperature range.

Keywords: Solid–liquid equilibrium; [emim][PF_6]; Phenylimidazole; DSC

1. Introduction

Room-temperature ionic liquids (RTILs) are low-melting organic salts built with an asymmetric, organic cation and an inorganic anion. RTILs are non-volatile, recyclable solvents, which exhibit a negligible vapour pressure and the electrical conductivity of an ionic conductor. Properties of these salts are dependent as well on the nature of the cation and the cation substituents as of that of the counteranions. RTILs are highly structured and oriented solvents, which impart selectivity in separation processes and in chemical reactions. These features infer a large domain of applications, such as replacement solvent [1–3], in organic synthesis, separation, extraction, and electrochemistry [3–9].

The phase equilibria of systems containing [emim][PF_6], has been extensively studied. The solubility of [emim][PF_6] in aromatic hydrocarbons (benzene, toluene, ethylbenzene, *o*-xylene, *m*-xylene and *p*-xylene) and in alcohols (methanol, ethanol, propan-1-ol, propan-2-ol, butan-2-ol, *tert*-butylalcohol and 3-methylbutan-1-ol) was reported as well as liquid–liquid equilibrium and solid–liquid equilibrium of aqueous solutions [10–12].

While previous studies on the RTILs solubility concerned essentially separation processes, the objective of this work is to assess consequences of the nanostructure organization of RTILs on thermodynamic properties of mixtures. With this view we have studied phase diagrams of systems formed by an imidazolium-based ionic liquid, 1-ethyl-3-methylimidazolium hexafluorophosphate [emim][PF_6], with substituted phenyl substituted imidazoles; 2-phenylimidazole, 4,5-diphenylimidazole and 2,4,5-triphenylimidazole. Both components of the mixtures studied contained the imidazole moiety. Chemical structures of the compounds studied are given in Fig. 1. Phenyl moiety in 2-phenylimidazole is more mobile as compared with 4,5-diphenylimidazole and 2,4,5-triphenylimidazole where the proximity of substituents hinders rotations. Consequently, the later molecules are more rigid and more compact. Therefore, increasing number of phenyl substituents should increase the ordering of imidazole molecules. 2,4,5-Triphenylimidazole does not form columnar liquid crystal structures, but it may be thought that the environment of the highly organised ionic liquid would induce a self-assembling of this compound.

Indeed, discotic liquid crystals based on imidazolium based ionic liquids were recently reported [13]. New liquid crystals were obtained by hybridization of self-organizing triphenylene discotics with imidazolium ionic liquids. Imidazolium-based ionic liquids were incorporated in the supramolecular order

---

* Corresponding author. Tel.: +33 387 31 54 34; fax: +33 387 54 74 62.
E-mail address: rogalski@univ-metz.fr (M. Rogalski).

0040-6031/$ – see front matter © 2007 Elsevier B.V. All rights reserved.
doi:10.1016/j.tca.2007.02.005

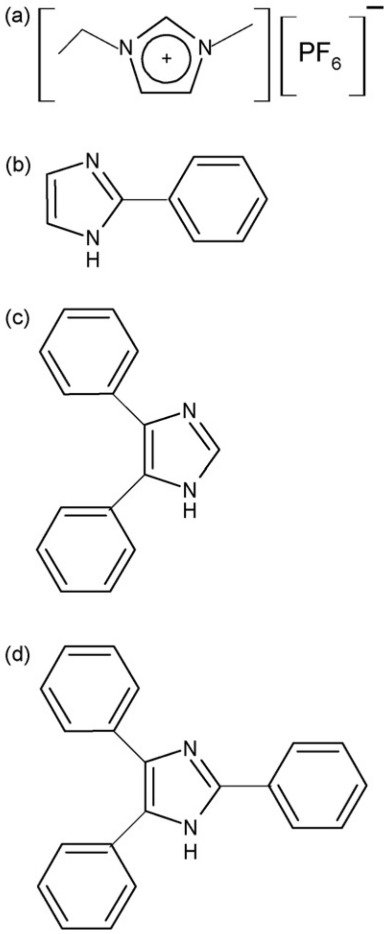

Fig. 1. Chemical structure of the compounds studied: (a) 1-ethyl-3-methylimidazolium hexaflurophosphate, (b) 2-phenylimidazole, (c) 4,5-diphenylimidazole, and (d) 2,4,5-triphenylimidazole.

of discotic liquid crystals by attaching triphenylene discotics covalently to the imidazolium salts.

During last years, the ionic liquid used in this study, [emim][PF_6], was one of the most widely studied ionic liquids. Spectroscopic methods has been used to confirm formation of the hydrogen bonding between ring and methyl hydrogen's and anions, with each cation surrounded by at least three anions and each anion surrounded by at least three cations [14]. While the anion is octahedral with nearly spherical symmetry, the cation is asymmetric that disturbs the charge ordering due to the ionic interactions. Therefore, [emim][PF_6] is a strongly organised compound with separated polar and non-polar domains [14].

We have studied the liquid–solid equilibrium of the systems: {[emim][PF_6] + 2-phenylimidazole}, {[emim][PF_6] + 4,5-diphenylimidazole} and {[emim][PF_6] + 2,4,5-triphenylimidazole}.

We think that the phase diagram pattern would be influenced by self-assembly occurring between two compounds of the mixture. While, mono and bi substituted imidazoles may probably incorporating the matrix of hydrogen bonded ionic liquid, 2,4,5-triphenylimidazole is expected to self-assembling in ionic liquid solution or co-assembly with imidazolium cations.

2. Experimental

2.1. Materials

Ionic liquid [emim][PF_6] was obtained from Solvent Innovation Gmbh, (Kölen, Germany) with a purity greater than 99% (w/w). 2-Phenylimidazole, 4,5-diphenylimidazole and 2,4,5-triphenylimidazole has been purchased from Sigma Aldrich and their purity was greater than 98% (w/w). All compounds were used as received without further purification.

2.2. Experimental methods

Calorimetric measurements were carried out using TA Instruments differential scanning calorimeter (DSC) model 2920 CE. The instrument was calibrated for temperature, and heat flow using high purity indium sample. The uncertainties of temperature and heat measurements were, respectively, ±0.3 °C and ±0.1 kJ/mol. The baseline was checked before each experiment by running the calorimeter with empty aluminium pans. Samples of 2–10 mg were weighted with accuracy of about ±0.005 mg and then placed in sealed, hermetic aluminium pans. Before measurement, samples were heated up to the temperatures higher than the melting temperatures of the mixture components and maintained during 15 min at this temperature. Then, they were cooled to the ambient temperature and equilibrated during 24 h at −10 °C. This thermal treatment was necessary to obtaining homogenous and crystalline samples.

All measurements were carried out with heating rate of 5 °C/min in inert atmosphere of argon gas (25 ml/min).

3. Results and discussion

Table 1 reports melting temperature, t_f, and enthalpy of fusion ΔH_f, of the compound studied determined in this work, or taken from the literature. The onset temperature of the thermal peak was taken as the melting temperature of pure compounds. Thermal curves of mixtures of different compositions are given in Figs. 2–4. These curves exhibiting two peaks

Table 1
Melting temperature, t_f, and enthalpy of fusion ΔH_f

Compound	t_f (°C)	ΔH_f (kJ mol^{-1})
[emim][PF_6]	60.9[a]	17.99[a]
	59.7[b]	17.86[b]
	62.0[c]	
2-Phenylimidazole	146.8[a]	17.81[a]
	149.7[d]	17.90[d]
4,5-Diphenylimidazole	231.8[a]	32.34[a]
	231.7[d]	34.19[d]
2,4,5-Triphenylimidazole	274.6[a]	37.31[a]
	277.6[d]	35.15[d]

[a] Determined in this work.
[b] Ref. [10].
[c] Ref. [15].
[d] Ref. [16].

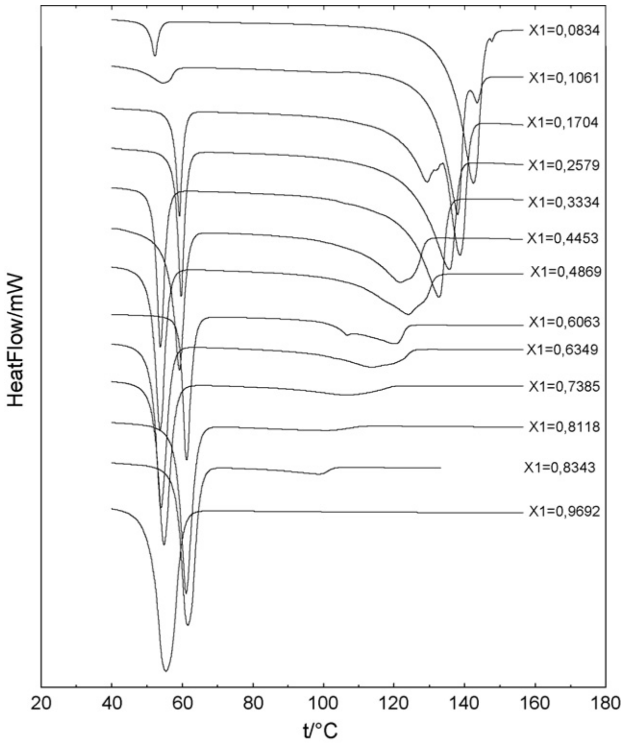

Fig. 2. Thermal curves of the system $\{[\text{emim}][\text{PF}_6] + \text{2-phenylimidazole}\}$.

with all composition studied indicate that both systems studied form simple eutectic diagrams. The onset temperature of the first peak was taken as the eutectic temperature. The second peak is wide and is split in two peaks for certain compositions. This behaviour is often observed in DSC measurements of the liquidus temperature. The maximum of the second peak (or of the sum of two peaks) was considered to be the liquidus temperature. Solubility data of $\{[\text{emim}][\text{PF}_6] + \text{2-phenylimidazole}\}$, $\{[\text{emim}][\text{PF}_6] + \text{4,5-diphenylimidazole}\}$ and $\{[\text{emim}][\text{PF}_6] + \text{2,4,5-triphenylimidazole}\}$ are reported, respectively, in Tables 2–4 together with activity coefficients of phenylimidazoles (in the case of two former systems) calculated with experimental data using equation:

$$\ln x_i = \frac{\Delta H_{\mathrm{f},i}}{R}\left[\frac{1}{t_{\mathrm{f},i}} - \frac{1}{t}\right] - \ln \gamma_i \tag{1}$$

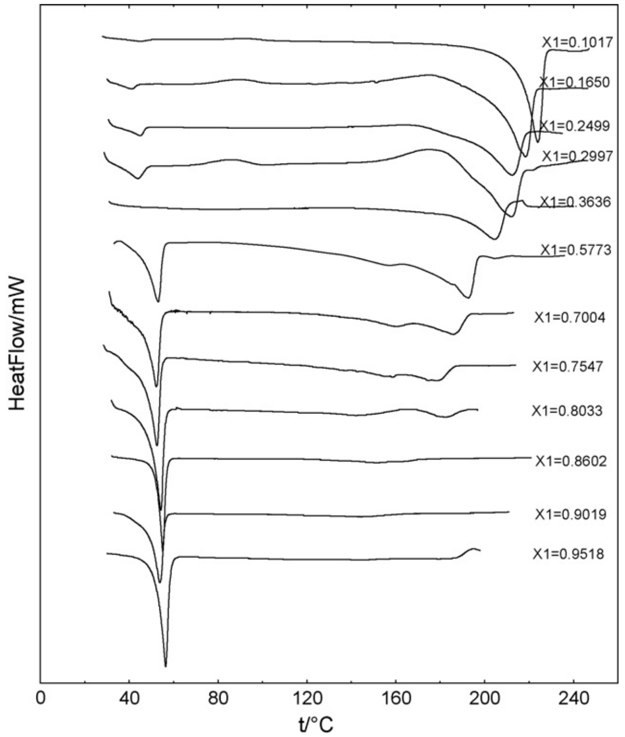

Fig. 3. Thermal curves of the system $\{[\text{emim}][\text{PF}_6] + \text{4,5-diphenylimidazole}\}$.

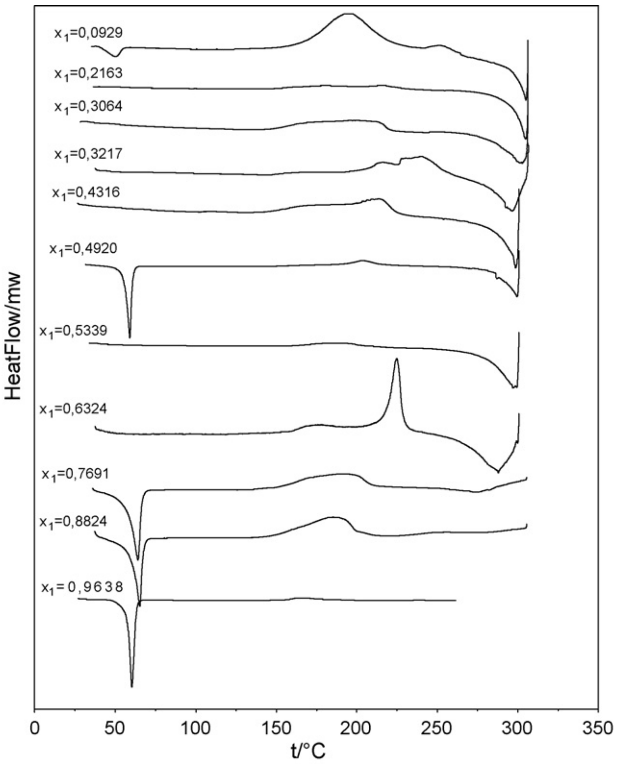

Fig. 4. Thermal curves of the system $\{[\text{emim}][\text{PF}_6] + \text{2,4,5-triphenylimidazole}\}$.

Table 2
Activity coefficient data and experimental data of the liquid–solid equilibrium of the system $\{x_1\ [\text{emim}][\text{PF}_6] + (1 - x_1)\ \text{2-phenylimidazole}\}$ x_1, t and γ_2 are, respectively, equilibrium composition, liquidus temperature and the activity coefficient of 2-phenylimidazole in liquid solution

x_1	t (°C)	γ_2
0.0834	142.5	1.032
0.1061	143.5	1.072
0.1704	138.7	1.085
0.2579	135.6	1.164
0.3334	132.8	1.247
0.4453	126.1	1.309
0.4869	124.1	1.435
0.6036	120.3	1.759
0.6369	114.0	1.750
0.7385	107.0	2.168
0.8118	101.3	2.183
0.8384	98.4	2.774
0.9692	55.4	3.105

Table 3
Activity coefficient data and experimental data of the liquid-solid equilibrium of the system $\{x_1$ [emim][PF$_6$] + $(1 - x_1)$ 4,5-diphenylimidazole$\}$ x_1, t and γ_2 are, respectively, equilibrium composition, liquidus temperature and the activity coefficient of 4,5-diphenylimidazole in liquid solution

x_1	t (°C)	γ_2
0.1017	223.9	0.985
0.1650	218.3	0.969
0.2499	212.2	0.976
0.2997	212.0	1.041
0.3636	204.4	1.009
0.4711	197.8	1.083
0.5773	192.9	1.243
0.7004	182.5	1.449
0.7547	176.6	1.581
0.8033	170.5	1.752
0.8602	155.4	1.808
0.9019	144.8	2.047
0.9518	116.0	2.092

The phase diagrams are showed in Figs. 5–7. The eutectic temperatures of {[emim][PF$_6$] + 2-phenylimidazole} and {[emim][PF$_6$] + 4,5-diphenylimidazole} were, respectively, $t_E = 53.9$ and $t_E = 43.3$ °C. The eutectic composition has been determined using the method proposed by Masuoka and Ozawa [17], and often used in the literature [18,19]. This method is based on the assumption that the eutectic fraction defined as:

$$f_E = \frac{\Delta H_E}{\Delta H_E + \Delta H_A} \tag{2}$$

is equal to one, $f_E = 1$, at the eutectic composition. ΔH_E and ΔH_A in Eq. (2) are, respectively, energy released at the eutectic temperature (first peak) and energy released above this temperature (second peak).

The values of the eutectic composition obtained with this method, illustrated in Fig. 8, were $x_{E,1} = 0.9368$ and $x_{E,1} = 0.9879$, for the first and the second system, respectively. The eutectic composition of the third system is very close to the pure ionic liquid and could not be precisely determined.

The phase diagrams of ideal systems were calculated using Eq. (1) without term of activity coefficient.

Table 4
Experimental data of the liquid–solid equilibrium of the system $\{x_1$ [emim][PF$_6$] + $(1 - x_1)$ 2,4,5-triphenylimidazole$\}$ x_1 and t are, respectively, equilibrium composition and liquidus temperature

x_1	t (°C)
0.0929	253.5
0.2163	253.0
0.3064	244.2
0.3217	245.2
0.4316	245.0
0.4920	245.5
0.5339	239.6
0.6324	230.6
0.7691	220.5
0.8824	186.6
0.9638	136.1

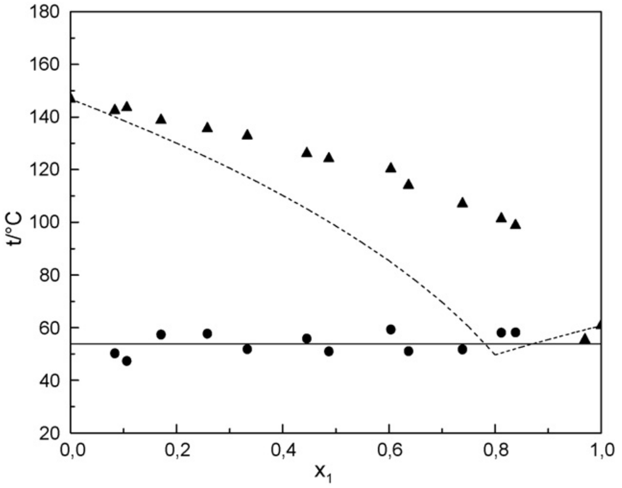

Fig. 5. SLE diagram of the system $\{x_1$ [emim][PF$_6$] + $(1 - x_1)$ 2-phenylimidazole$\}$; (▲) liquidus temperature, (●) eutectic temperature, (- - -) liquidus curve corresponding to the ideal system.

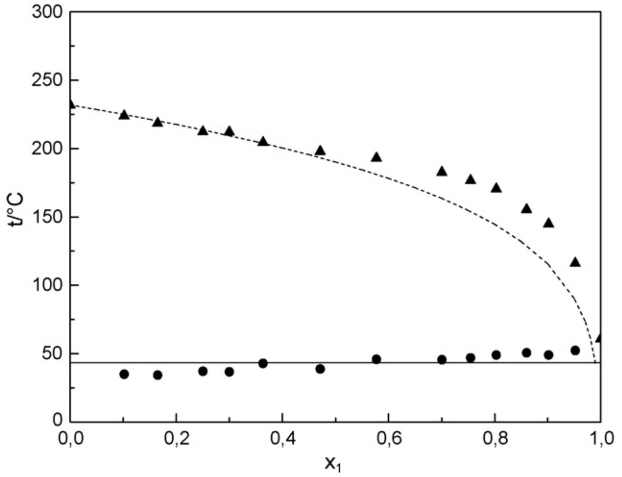

Fig. 6. SLE diagram of the system $\{x_1$ [emim][PF$_6$] + $(1 - x_1)$ 4,5-diphenylimidazole$\}$; (▲) liquidus temperature, (●) eutectic temperature, (- - -) liquidus curve corresponding to the ideal system.

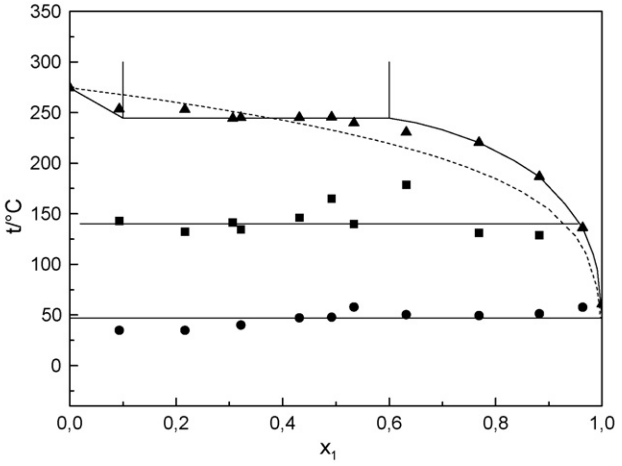

Fig. 7. SLE diagram of the system $\{x_1$ [emim][PF$_6$] + $(1 - x_1)$ 2,4,5-triphenylimidazole$\}$; (▲) liquidus temperature, (●) eutectic temperature, (■) exothermic effect temperature, (- - -) liquidus curve corresponding to the ideal system. The phase splitting domain is marked with vertical lines.

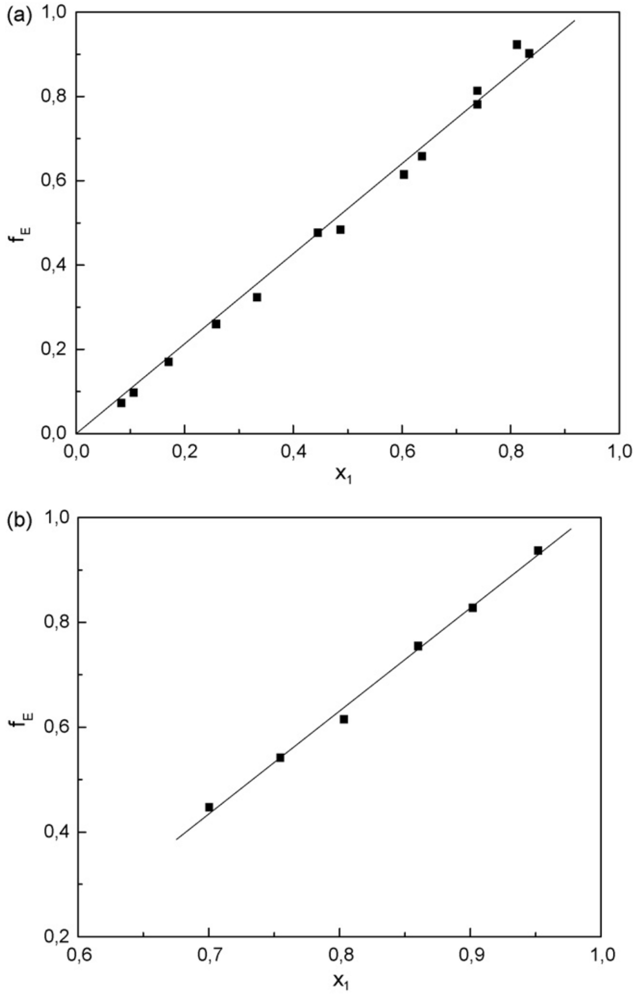

Fig. 8. Determination of the eutectic composition according to the Masuoka method—plot of the eutectic fraction, f_E, in composition for: (a) $\{x_1[\text{emim}][\text{PF}_6] + (1-x_1)$ 2-phenylimidazole$\}$ and (b) $\{x_1[\text{emim}][\text{PF}_6] + (1-x_1)$ 4,5-diphenylimidazole$\}$.

The analysis of the phase diagrams of three systems leads to several observations:

1. System $\{[\text{emim}][\text{PF}_6] + 2\text{-phenylimidazole}\}$ is more non-ideal than the system$\{[\text{emim}][\text{PF}_6] + 4,5\text{-diphenylimidazole}\}$. The second system is nearly ideal at concentrations of the ionic liquid smaller than $x_1 = 0.5$.
2. Both systems are highly non-ideal at concentrations $x_1 > 0.5$. Activity coefficient of 2-phenylimidazole rises steeply, Fig. 9, and attains the value of three at $x_1 = 0.8$. The probable value of the activity coefficient at infinite dilution exceeds four. The activity coefficient of 4,5-diphenylimidazole is lower, Fig. 10, but behaves in a similar way in this concentration range.
3. Analytical representation of activity coefficients of 2-phenylimidazole and 4,5-diphenylimidazole necessitates at least four parameters of the Redlich–Kister polynomial [20]. This representation has purely correlative character. Indeed, activity coefficients were measured at different temperatures. Moreover, they take into account the structural changes occurring in the mixture studied with increasing temperature.

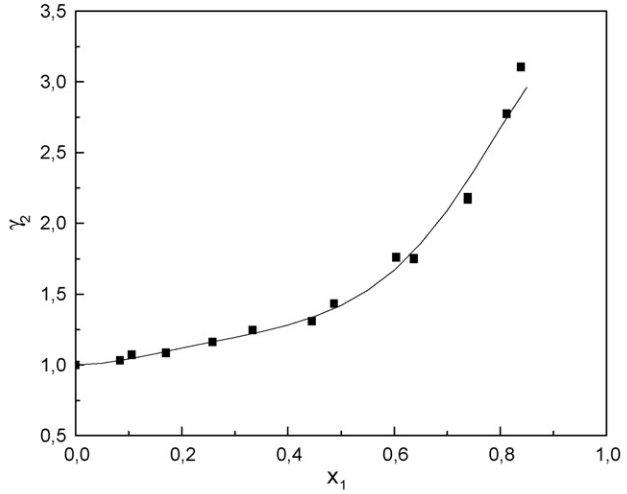

Fig. 9. Activity coefficient of 2-phenylimidazole calculated using Eq. (1). Redlich–Kister equation was used to calculating $\gamma_2(x_1)$: $\ln\gamma_2 = x_1^2(6.0189 - 22.4836x_1 + 35.5323x_1^2 - 18.0383x_1^3)$.

4. System $\{[\text{emim}][\text{PF}_6] + 2,4,5\text{-triphenylimidazole}\}$ displays a phase splitting at high temperatures. The location of the two phase domain is indicated in Fig. 7.
5. System $\{[\text{emim}][\text{PF}_6] + 2,4,5\text{-triphenylimidazole}$ exhibits an exothermic transition at temperature of about 140 °C as can be seen in Fig. 7.
6. The melting temperature of 2,4,5-triphenylimidazole exceeds the starting temperature of decomposition of the ionic liquid that is of 235 °C.

Phenomena reported in points 4 and 6 make that activity coefficients of 2,4,5-triphenylimidazole in $\{[\text{emim}][\text{PF}_6] + 2,4,5\text{-triphenylimidazole}\}$ mixture cannot be calculated with the liquidus curve.

Above discussed features of phase diagrams confirm our hypothesis formulated in introduction to this paper. Interactions of phenylimidazoles with the highly hydrogen bonded matrix of

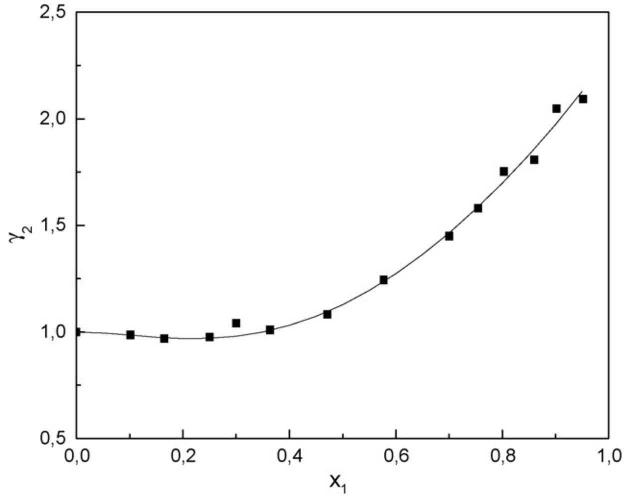

Fig. 10. Activity coefficient of 4,5-diphenylimidazole calculated using Eq. (1). Redlich–Kister equation was used to calculating $\gamma_2(x_1)$: $\ln\gamma_2 = x_1^2(-2.4361 + 10.2088x_1 - 10.5603x_1^2 + 3.6220x_1^3)$.

the ionic liquid strongly depend on the molecular structure of these compounds. The most flexible 2-phenylimidazole displays smaller capability to inserting the ionic liquid matrix. Smaller activity coefficient of 4,5-diphenylimidazole indicates that this more ordered molecule integrates the ionic liquid structure easier. The third system displays the most complex behaviour. We observed the phase splitting occurring at high temperatures. The first phase is liquid and the second one is a viscous, oily dispersion. We think that exothermic transition observed at 140 °C corresponds to formation of a mesophase built with both components of the mixtures. This mesophase would be one of two phases stable above the melting point of 2,4,5-triphenylimidazole. The formation of this mesophase is possible at high temperatures were hydrogen bonding between the anion and cation of the ionic liquid weakens. Unfortunately, due to high temperature range considered, it is difficult to confirm this hypothesis with other techniques.

4. Conclusions

The phase behaviour and heat effects observed in three mixture studied suggest that the solubility in ionic liquids depends of interactions between the solute and the solvent network and not with the solvent molecules. This type of interactions was observed and described in the case of solute–liquid crystal solutions [21].

At high temperatures 2,4,5-triphenylimidazole forms probably a mesophase in ionic liquid solution.

Acknowledgement

One of us (H.S.) thanks the Ministère de l′Enseignement Supérieur et de la Recherche Scientifique Algerien, Algeria, for the financial support.

References

[1] K.R. Seddon, J. Chem. Tech. Biotec. 68 (1997) 351–356.

[2] R.A. Sheldon, The role of catalysis in waste minimization, in: M.P.C. Weijnem, A.A.H. Drinkenburg (Eds.), Precision Process Technology, Perspectives for Pollution Prevention, Kluwer, Dodrecht, 1993.

[3] S.G. Cull, J.D. Holbery, V. Vargas-Mora, K.R. Seddon, G.J. Lye, Biotechnol. Bioeng. 69 (2000) 227–233.

[4] S.W. John, J. Mol. Catal. A: Chem. 214 (2004) 11–17.

[5] P. Wasserschlid, W. Keim, Angew. Chem. Int. Ed. 39 (2000) 3773–3789.

[6] T. Welton, Chem. Rev. 99 (1999) 2071–2083.

[7] J.F. Brennecke, E.J. Maginn, AIChE J. 47 (2001) 2384–2389.

[8] C.P. Fredlake, J.M. Crosthwaite, D.G. Hert, S.N.V.K. Aki, J.F. Brennecke, J. Chem. Eng. Data 49 (2004) 954–964.

[9] A.H. Wesley, P. Stefano, Chem. Mater. 16 (2004) 2881–2885.

[10] U. Domanska, A. Marciniak, J. Chem. Eng. Data 48 (2003) 451–456.

[11] U. Domanska, A. Marciniak, J. Phys. Chem. B 108 (2004) 2376–2382.

[12] S.H.W. David, P.C. Jia, M.C. Jyh, H.C. Cheng, Fluid Phase Equilibria 194–197 (2002) 1089–1095.

[13] C. Thomas, D. Kris, N.P.-V Tatjana, H. Benoit, B. Cyril, G. Daniel, D. Bertrand, B. Koen, Chem. Mater. 17 (2005) 6589–6598.

[14] N.A.C.L José, A.H.P. Agilio, J. Phys. Chem. B 110 (2006) 3330–3335.

[15] H.L. Ngo, K. LeCompte, L. Hargens, A.B. McEwen, Thermochim. Acta 357–358 (2000) 97–102.

[16] U. Domanska, A. Pobudkowska, M. Rogalski, J. Chem. Eng. Data 49 (2004) 1082–1090.

[17] M. Masuoka, R. Ozawa, J. Cryst. Growth 96 (1989) 596–604.

[18] H. Cheng-Chia, C. Yan-Ping, Chem. Eng. Sci. 55 (2000) 3175–3185.

[19] C. Yan-Ping, T. Muoi, K. Ju-Chia, Fluid Phase Equilibria 232 (2005) 182–188.

[20] O. Redlich, A.T. Kister, Ind. Eng. Chem. 40 (1948) 341–345.

[21] M. Badis, M.H. Guermouche, M. Rogalski, J.P. Bayle, E. et Rogalska, Langmuir 20 (2004) 7991–7997.